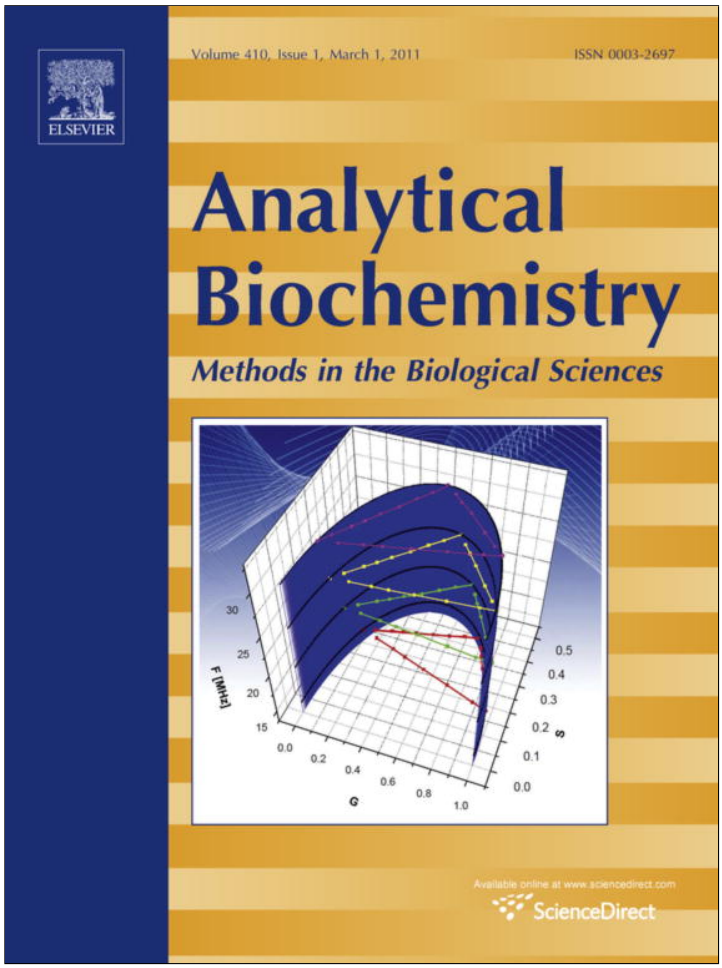

Analytical Biochemistry 410 (2011) 118–123

Contents lists available at ScienceDirect

Analytical Biochemistry

journal homepage: www.elsevier.com/locate/yabio

Infrared study of trifluoroacetic acid unpurified synthetic peptides in aqueous solution: Trifluoroacetic acid removal and band assignment

Laura E. Valenti, Maximiliano Burgos Paci, Carlos P. De Pauli, Carla E. Giacomelli *

INFIQC–Departamento de Fisicoquímica, Facultad de Ciencias Químicas, Universidad Nacional de Córdoba, CP 5000 Córdoba, Argentina

ARTICLE INFO

Article history:
Received 24 August 2010
Received in revised form 4 November 2010
Accepted 5 November 2010
Available online 13 November 2010

Keywords:
ATR–IR
Hexahistidine
TFA subtraction
Semiempirical calculations
Band assignment

ABSTRACT

Synthetic peptide or protein samples are mostly unpurified with trifluoroacetic acid (TFA) used during the synthesis procedure, which strongly interferes with structure determination by infrared (IR) spectroscopy. The aim of this work was to propose a simple strategy to remove TFA contribution from attenuated total reflection (ATR)–IR spectra of the hexahistidine peptide (His6) in aqueous solution to study the conformation of this synthetic peptide without previous purification. Such a strategy is based on the subtraction mode widely employed to remove water contribution, and it is tested with TFA unpurified histidine as a model system. The subtraction is based on eliminating the strong TFA bands at 1147 and 1200 cm^{-1} by applying a scaling factor (as in buffer correction). The proposed modes represent excellent strategies that do not modify spectral features, and they provide reliable routines to obtain the synthetic peptide spectrum without TFA contribution. The conformational information from the corrected spectra at different pH values is deduced from semiempirical calculated IR spectra of different His6 conformers. The spectral features and the band positions of the corrected spectrum suggest that the peptide molecules mainly adopt an intermolecular β-sheet structure.

Synthetic techniques to produce short peptides and proteins allow obtaining peptides that are difficult to express in bacteria, adding artificial amino acids to a natural sequence, and modifying the peptide or protein backbone. The most employed technique with such goals is solid phase synthesis, in which the peptide chain polymerizes bonded to a solid surface [1,2]. After the synthesis, trifluoroacetic acid (TFA)[1] is used to cleave the peptide chain from the surface, and it is usually added to the purification buffer, commonly performed by high-performance liquid chromatography (HPLC) [3,4]. Thus, synthetic peptide or protein samples are mostly unpurified with TFA, which strongly interferes with the structure determination by infrared (IR) spectroscopy [5].

The amide I band (mainly peptide bond C=O stretching vibration), usually analyzed to determine the secondary structure of peptides and proteins, appears between 1600 and 1700 cm^{-1} and strongly overlaps with the H_2O bending vibration at 1640 cm^{-1} [6]. Because the intensity of this water vibration is approximately an order of magnitude higher than the amide I band, aqueous samples demand a short path length to avoid subtraction inaccuracy. In the attenuated total reflection (ATR) technique, the path length is very short (~1 μm) [7], and it is widely used to study peptide and protein conformation in aqueous solution. Besides, the presence of TFA in solution also contributes to this region because of the strong vibration of the COO^- group at 1673 cm^{-1} [8]. Due to this interference, some authors have stated that it is not possible to analyze the secondary structure of synthetic peptides by IR without a previous purification from TFA [9–11]. In other cases, the TFA contribution has been erroneously included as a part of the amide I band [12].

TFA removal from synthetic samples has been performed by means of various procedures such as washing with dialysis membrane, lyophilization in the presence of HCl, and chromatography. Usually, peptide lyophilization from 0.1 M HCl solution is preferred due to its simplicity and high peptide yield after purification [13]. Nevertheless, high HCl concentrations may modify the peptide structure and reduce its thermal stability, thereby interfering with subsequent conformational studies. Hence, lower HCl concentrations have also been tested to remove TFA, minimizing the peptide secondary structure perturbation [5,14,15]. Although this purification technique is rather simple, it is time-consuming because the sample must be lyophilized several times [16]. Thus, a simple strategy to remove the TFA contribution from IR spectra without purifying the commercially available peptide or protein sample is greatly needed to easily collect conformational information.

The aim of this work was to propose a simple strategy to remove the TFA contribution from ATR–IR spectra of the hexahistidine

* Corresponding author. Fax: +54 351 4334188.
E-mail address: giacomel@fcq.unc.edu.ar (C.E. Giacomelli).

[1] *Abbreviations used:* TFA, trifluoroacetic acid; HPLC, high-performance liquid chromatography; IR, infrared; ATR, attenuated total reflection; His6, hexahistidine peptide; FTIR, Fourier transform-infrared; PES, potential energy surface; Blk, blank; FSD, Fourier self-deconvolution.

0003-2697/$ - see front matter © 2010 Elsevier Inc. All rights reserved.
doi:10.1016/j.ab.2010.11.006

peptide (His6) in aqueous solution to study the conformation of this synthetic peptide without previous purification. This strategy is based on the subtraction mode widely employed to remove the water contribution, and it was tested with TFA unpurified histidine as a model system. The conformational information from the corrected spectra at different pH values was deduced from semiempirical calculated IR spectra of different His6 conformers.

Materials and methods

Materials

L(+)Histidine (His) was purchased from Anedra (98.9% purity), and hexahistidine (His6) was purchased from New England Peptide (98.4% purity and 50–90% net peptide content) (TFA salts are the main nonpeptide components). Both samples were used without further purification. The reactants $NaH_2PO_4 \cdot 7H_2O$ (Baker) and TFA (Baker) were of analytical grade. Aqueous solutions were prepared using 18 MΩ/cm resistance water (Milli-Q, Millipore). All of the experiments were performed at room temperature (25 ± 2 °C).

Phosphate buffer was prepared by dissolving the desired amount of NaH_2PO_4 in water to reach a 5-mM concentration and adjusting the pH with either 2 M NaOH (Baker) or 2 M HCl (Baker). pH measurements were performed with a combined glass electrode and a digital pH meter (Orion 420A+, Thermo). Pure and unpurified histidine, commercially available His6, and TFA solutions were prepared by adding the appropriate amount to 5 mM phosphate buffer at pH values of 4.0, 6.0, and 8.0. Different concentrations of pure His (100, 25, and 6.25 mM), TFA (4.00×10^{-1}, 1.00×10^{-1}, 5.00×10^{-2}, 2.50×10^{-2}, and 1.25×10^{-2}%, w/v), and His6 (1.25, 2.5, and 10 mg/ml) solutions were used. Unpurified histidine (His + TFA) solutions were prepared by mixing these TFA and His solutions to reach concentrations ranging from (100 mM His + 4.00×10^{-1}% [w/v] TFA) to (6.25 mM His + 1.25×10^{-2}% [w/v] TFA).

Methods

ATR–FTIR (Fourier transform infrared) spectra were collected with an FTIR Nicolet Magna 560 spectrometer with a DTGS detector using a triangular apodization function. The FTIR spectrometer was continuously purged with H_2O/CO_2 free air. The sample solution (His, TFA, His + TFA, or His6) was placed in a horizontal ATR accessory (Thermo Nicolet) with a germanium prism. All spectra were obtained with 1000 scans and at a 2-cm^{-1} resolution. The blank spectrum—buffer solution—was collected before each measurement with the same accessory and in the same instrumental conditions as the sample. The equipment software (OMNIC 7.3, Thermo Electron) was employed to manipulate and analyze the spectra.

Semiempirical methods using the AM1 force field were employed to calculate the IR spectra of selected conformers in the gas phase. Due to the enormous number of degrees of freedom of the system and the complexity of the potential energy surface (PES) of His6, a model to scan it and pick a representative group of conformers is needed. The goal in the current case is to obtain a qualitative reference for the assignment of the IR spectra, and the most important differences in the band positions at the experimental spectral window are due to the backbone conformations. Hence, the first step was to optimize the allowed regular conformations of the zwitterions. PES minima were confirmed checking for no imaginary frequencies in the Hessian matrix. From the optimized structures, the group of the most stable conformers (left α-helix, $helix_{3-10}$, β-sheet, and β-turn) was chosen for the analysis of the vibrational modes. The vibrational intensities were scaled with the Boltzmann factor corresponding to each structure, and the assignment was performed analyzing the components of the displacement vibrational vectors and with the help of the GaussView visualizing software (GaussView 4.1, Gaussian). All of the calculations were run with the Gaussian03 program suite [17].

Results and discussion

Model system: subtraction strategy with TFA unpurified His

Fig. 1 shows the blank corrected spectra of 4.00×10^{-1}% (w/v) TFA (Blk–TFA), 100 mM His (Blk–His), and 100 mM His + 4.00×10^{-1}% (w/v) TFA (Blk–His + TFA) solutions at pH 8.0. In the figure, the curves are shifted in the *y* axis for the sake of clarity. The buffer contribution was completely removed by using a scaling factor on the blank spectrum with an iterative procedure until the baseline between 1800 and 1900 cm^{-1} was flat in the corrected spectrum [7]. Both His and TFA absorb in the 1300- to 1700-cm^{-1} region. The latter also presents bands in the 1100- to 1300-cm^{-1} range that have been erroneously assigned to the mainly predominant C—N stretching bands of hexapeptides [12]. Thus, the spectrum of unpurified His presents extra features when compared with that of pure His: a shoulder at 1673 cm^{-1} and two strong absorption bands at 1147 and 1200 cm^{-1}. Because the main absorption bands in proteins and peptides appear above 1200 cm^{-1} [6], the strong TFA bands at 1147 and 1200 cm^{-1} provide a clean reference to quantify its concentration and to remove its contribution from the spectrum of unpurified samples.

To find a suitable subtraction strategy to remove TFA contribution from the spectrum of unpurified peptide samples, two modes are first analyzed: (1) (His + TFA) spectrum − (TFA) spectrum and (2) (Blk–His + TFA) spectrum − (Blk–TFA) spectrum. In mode 1, TFA and buffer contributions are eliminated in one operation, whereas it is necessary to subtract three times to achieve the same result by using mode 2. The latter mode is preferable when the spectra are collected in independent measurements (e.g., different solutions) or using different buffer solutions. Both subtraction modes are based on eliminating the strong TFA bands at 1147 and 1200 cm^{-1} by applying a scaling factor (as performed with the blank correction).

Fig. 2A compares the subtraction modes applied to the 100-mM His + 4.00×10^{-1}% (w/v) TFA spectrum. To verify their capabilities, the 100-mM Blk–His spectrum is also included in the figure. Spectra are shifted in the *y* axis for the sake of clarity. The results

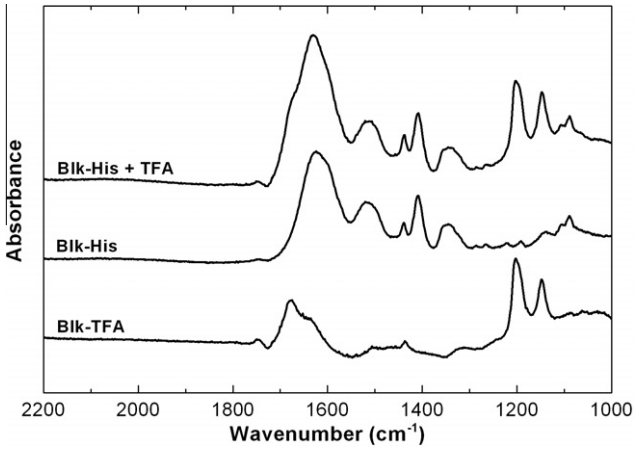

Fig.1. ATR–FTIR blank corrected spectra of 4.00×10^{-1}% (w/v) TFA (Blk–TFA), pure 100 mM histidine (Blk–His), and unpurified (100 mM His + 4.00×10^{-1}% [w/v] TFA) histidine (Blk–His + TFA) collected in aqueous solution at pH 8.0.

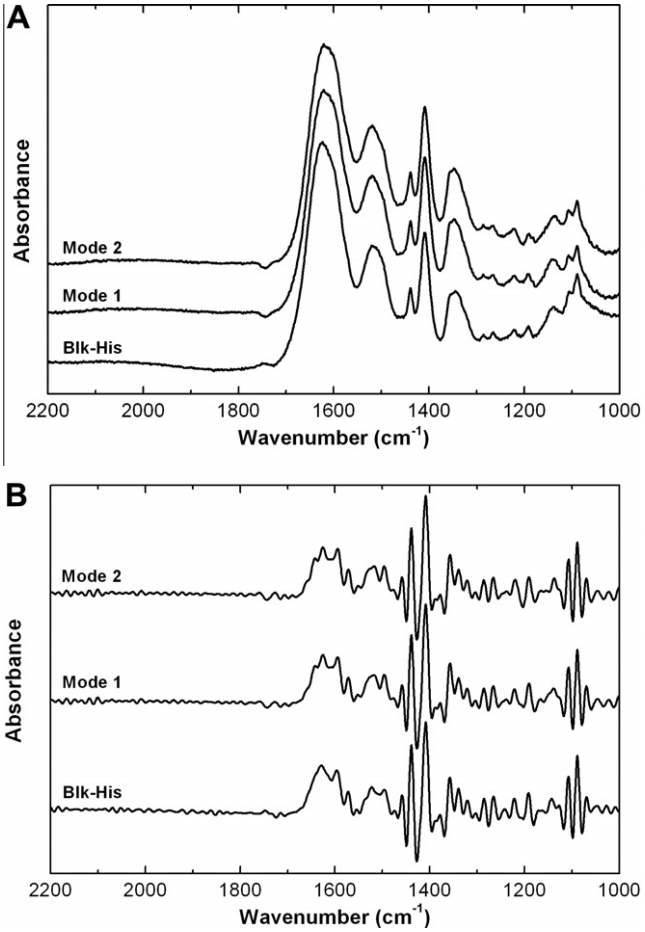

Fig.2. (A) ATR–FTIR blank corrected spectrum of pure 100 mM histidine (Blk–His) and TFA subtracted spectra of unpurified histidine (100 mM His + 4.00 × 10^{-1}% [w/v] TFA) by modes 1 and 2. (B) Fourier self-deconvolution (FSD) of the spectra in panel A.

indicate that the corrected His + TFA and the pure His spectra are equivalent. Moreover, as shown in Fig. 2B, Fourier self-deconvolution (FSD) analysis gives the same band positions for the three spectra displayed in Fig. 2A. As reported elsewhere, the main His bands observed at pH 8.0 correspond to the following [18]:

- band at 1623 cm^{-1} composed of the COO^- antisymmetric stretching (1570 cm^{-1}) and the NH_3^+ antisymmetric bending vibrations (1629 cm^{-1});
- band at 1520 cm^{-1} composed of the ring stretching and the NH_3^+ symmetric bending (1521 cm^{-1}) overlapped with the in-plane N—H bending and the C=N bending vibrations (1496 cm^{-1});
- CH_2 bending at 1438 cm^{-1};
- COO^- symmetric stretching at 1408 cm^{-1};
- CH_2 vibrations at 1345 cm^{-1}; and
- ring vibrations below 1300 cm^{-1}.

Both modes represent excellent subtraction strategies without modifying the spectral features or removing or adding new bands, and they provide reliable routines to obtain the His spectrum without either water or TFA contribution.

To check the reliability of the subtraction, modes 1 and 2 were also applied to spectra measured at different TFA and His concentrations and pH values (data not shown). The corrected His + TFA and pure His spectra were equivalent for the following unpurified solutions: 100 mM His + 4.00 × 10^{-1}% (w/v) TFA, 100 mM His + 1.00 × 10^{-1}% (w/v) TFA, 100 mM His + 5.00 × 10^{-2}% (w/v) TFA, 25 mM His + 4.00 × 10^{-1}% (w/v) TFA, and 25 mM His + 1.00 × 10^{-1}% (w/v) TFA. Lower concentrations of either His or TFA prevent a reliable subtraction. For this reason, a concentration higher than 10 mM (by residue) of the synthetic peptide is desirable to properly remove the TFA contribution. On the other hand, TFA absorbance at 1147 or 1200 cm^{-1} is too low at concentrations lower than 1.00 × 10^{-1}% (w/v) to attain a reliable subtraction. The subtraction output was not affected by varying the pH from 8.0 to 4.0. The TFA spectrum does not change in this pH range, and the same characteristic bands are used to remove its contribution.

To use either subtraction mode, it is crucial to have a TFA spectrum with the same concentration as its content in the unpurified sample. Although TFA concentration may be estimated from the provider data, an accurate concentration is needed to properly subtract its spectral features. As indicated previously, TFA bands at 1147 and 1200 cm^{-1} do not overlap with any protein or peptide vibration, allowing a direct determination of the sample TFA content. Fig. 3 shows the linear relationship between the absorbance (A) at 1200 cm^{-1} and TFA concentration ([TFA]): $A = 1.87 \times 10^{-2} \times$ [TFA] (%, w/v) + 5.8 × 10^{-4} ($R^2 = 0.9989$). To perform this calibration curve, the absorbance values were measured from TFA spectra without subtracting the buffer contribution. The baseline was automatically calculated (OMNIC software) in the 1100- to 1250-cm^{-1} range; this correction causes the small y intercept in the calibration curve. Finally, it is worth noting that the absorbance of the band at 1147 cm^{-1} also gives a good calibration curve (data not shown). However, the results obtained at 1200 cm^{-1} allow a better correlation and sensitivity.

Studied system: TFA unpurified His6 sample

Fig. 4 depicts the blank corrected spectra of a 2.5-mg/ml commercially available His6 sample before (Fig. 4A) and after (Fig. 4B) subtracting the TFA contribution measured in aqueous solution at pH values of 4.0, 6.0, and 8.0. For the sake of clarity, the spectra are shifted in the y axis. Before correction, they present strong absorption bands in the 1700- to 1500-cm^{-1} range due to the hexapeptide and TFA vibration modes. As expected, bands in the 1200- to 1100-cm^{-1} region are also present and are due to TFA. Although the spectra shown in Fig. 4B were obtained with subtraction mode 2, equivalent spectra were achieved with mode 1. To correct the spectra of the commercially available His6 sample, mode 2 is preferred because it provides a more general subtraction mode.

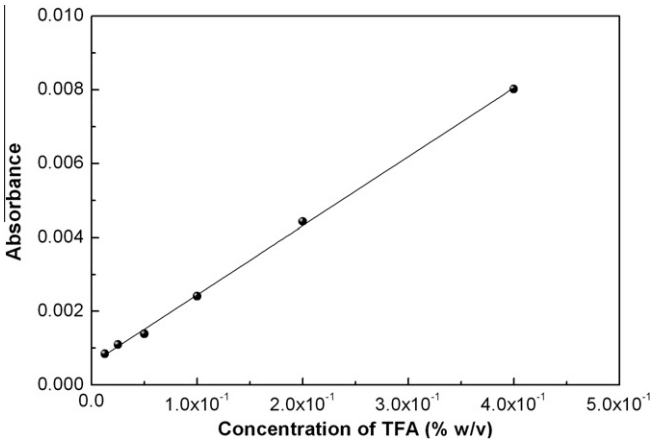

Fig.3. Correlation between the absorbance (A) of the 1200-cm^{-1} band and the TFA concentration ([TFA]): $A = 1.87 \times 10^{-2} \times$ [TFA] (%, w/v) + 5.8 × 10^{-4} ($R^2 = 0.9989$).

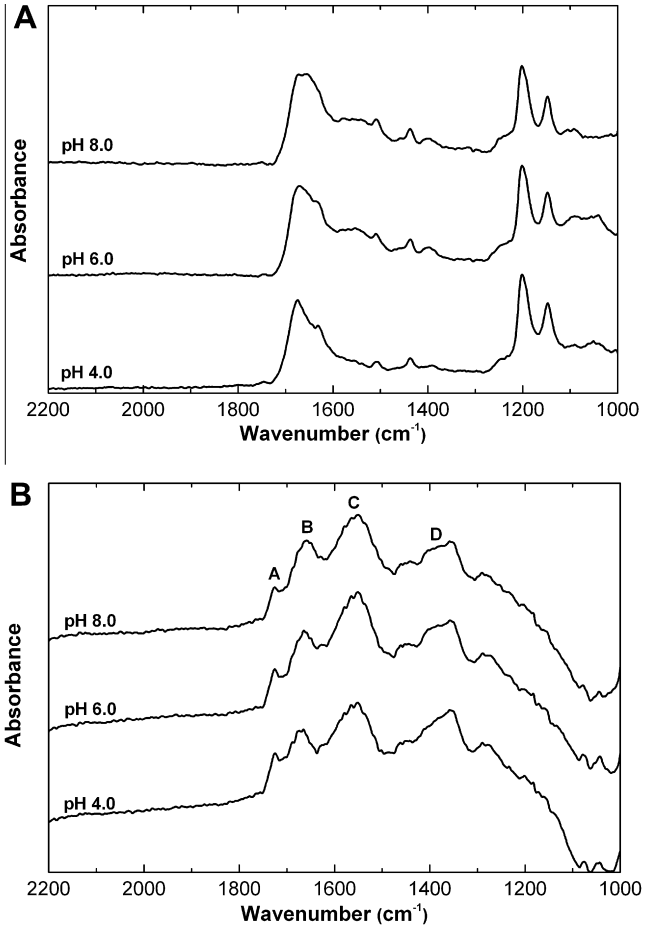

Fig.4. ATR–FTIR blank corrected spectra of 2.5 mg/ml commercially available before (A) and after (B) TFA subtraction collected in aqueous solution at pH values of 4.0, 6.0, and 8.0.

Determining the actual TFA content in the commercially available sample is the first step to removing its contribution from the peptide spectrum. Hence, the absorbance at 1200 cm^{-1} of the sample spectrum (after an automatic baseline correction between 1100 and 1250 cm^{-1}) and the calibration curve (Fig. 3) are used to measure TFA concentration: 0.13% and 0.56% (w/v) for the 2.5- and 10-mg/ml samples, respectively. At sample concentrations lower than 2.5 mg/ml, the absorbance of the band at 1200 cm^{-1} is too low to properly assess TFA content. Once the TFA concentration is known, water and TFA contributions are removed in the spectral region where the hexapeptide also absorbs. For doing that, both the buffer spectrum and the TFA one at the appropriate concentration are needed. Clearly, the spectra presented in Fig. 4B do not show the 1147- and 1200-cm^{-1} bands corresponding to TFA, demonstrating that its contribution is completely removed. Thus, the spectral features displayed in Fig. 4B belong only to His6 at different pH values.

His6 structure: Band assignment by semiempirical calculation

The band assignment of the experimental spectra is based on semiempirical calculations performed at different His6 conformations and comparison with bibliographic references. Fig. 5 shows the calculated IR spectra of four different hexapeptide conformers: left α-helix, $helix_{3-10}$, β-sheet, and β-turn. In the calculated spectra, both the individual vibration signals and the enveloping bands are shown as a function of the corrected wavenumber. The absorption bands in the calculated spectrum appear at higher energy than those corresponding to the experimental ones, and this can be thought of as a systematic shift due to the solvent effect. On these grounds, the *x* axes of the calculated spectra are corrected to match the absorption energy of the experimental bands. The same correction is applied to the four conformer spectra. The letters A to D are the references for the band assignment listed in Table 1. It is worth noting that regardless of the type of conformer, the signals arise in the same order of energy, although varying slightly in position. For all of the conformers considered, the first signal that appears at the highest energy belongs to the COO^- antisymmetric stretching vibration (C terminal, ν_{as} COO^-), followed by the amide I band, and so on. Thus, the reference letters (A–D) name a group of vibrations that, in general, appear in the same enveloping band irrespective of the His6 conformation.

Calculations indicate that the most intense signals belong to the vibration of the ν_{as} COO^-, the NH_3^+ antisymmetric bending (N terminal, δ_{as} NH_3^+), and the amide I and II vibrations. However, the relative intensity and the precise position of each vibration cause enveloping bands with different bandwidth. Moreover, A and B bands are either overlapped or resolved depending on the conformer. Calculations show that these spectral features are due to the position of the amide I band, which is strongly affected by the peptide conformation (1657 cm^{-1} left α-helix, 1700 cm^{-1} $helix_{3-10}$, 1675 cm^{-1} intermolecular antiparallel β-sheet, and 1668 cm^{-1} β-turn). The calculated vibrations of the amide I bands are in agreement with published results [19,20].

The experimental spectra shown in Fig. 4B also present four main bands that follow the energy sequence obtained from the semiempirical calculations. Hence, the experimental and calculated enveloping bands belong to the same group of vibrations, and they are named with the same reference letters (A–D, Table 1). However, as expected, the experimental bands are wider than the theoretical ones, causing strong overlapped spectra. Based on the semiempirical calculation, the experimentally observed band A (1725 cm^{-1}) is assigned to the His6 ν_{as} COO^- vibration, although the position does not correspond to the same vibration in histidine (1570 cm^{-1} [see Fig. 2]). This disagreement may be due to two opposite effects: (i) the overlap between the ν_{as} COO^- and δ_{as} NH_3^+ vibrations in histidine, in particular [18], and in amino acids, in general [21], shifts the COO^- vibration to lower wavenumbers; (ii) the interaction between charged C and N terminal and/or the exposure of carboxylate to the aqueous solution in His6 shift the vibration to higher wavenumbers [12,22]. The experimental band B (1660–1675 cm^{-1} depending on the pH) is easily assigned to the amide I band, related to intermolecular/antiparallel β-sheet structure in short peptides [12,23]. The experimentally observed band C is due mainly to the amide II band (1552 cm^{-1}) and the cationic amino vibrations (~1560 cm^{-1}), in very good agreement with reported results for histidine and short peptides [24]. Finally, band D (~1360 cm^{-1}) corresponds to the amide III band, as indicated by the calculations and reported in the literature [25,26], and to the vibrations of the imidazole ring, also observed in the histidine spectrum (Fig. 2).

A comparison between the experimental and calculated spectra suggests that His6 does not adopt a preferred conformation. However, the amide I position (band B) and the main spectral features of the experimental spectra are more related to the β-sheet conformer than to the other ones. In the studied pH range, both terminal groups of the hexapeptide molecules are ionized, whereas the charge of the side chain depends on the pH: from three protonated imidazole rings at pH 4.0 to neutral side chains at pH 8.0 [27]. The position of the amide I band at pH 4.0 corresponds to a regular antiparallel/intermolecular β-sheet (1675 cm^{-1} [23]) structure. This conformation may arise from two main contributions that promote and stabilize intermolecular interactions. First, the attrac-

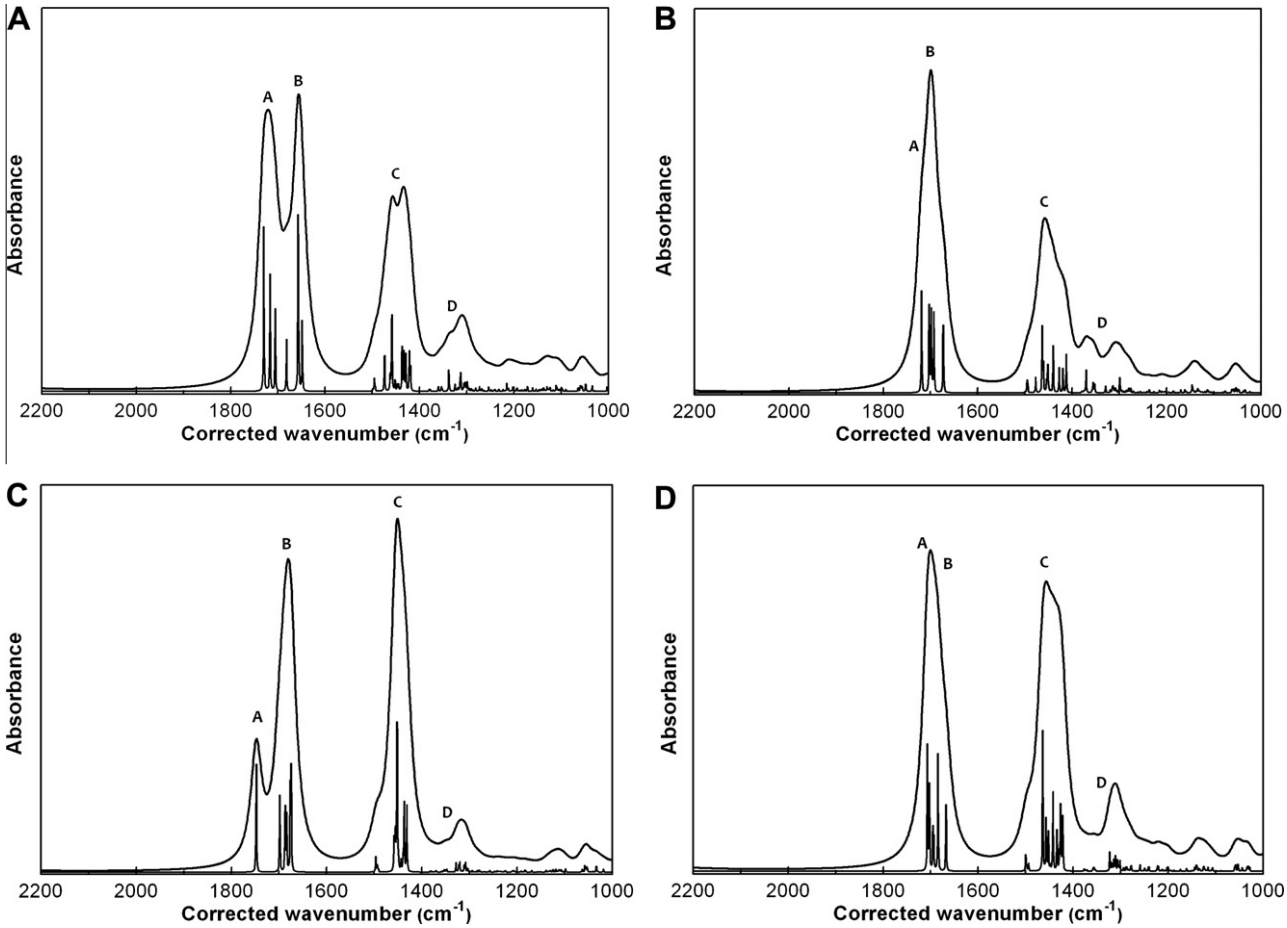

Fig.5. Calculated IR spectra of different His6 conformers: (A) left α-helix; (B) helix$_{3-10}$; (C) β-sheet; (D) β-turn. The letters A to D are the references for the band assignment listed in Table 1.

Table 1
Calculated bands for the different conformers of His6 spectra (Fig. 5) and band assignments for the experimental spectra (Fig. 4).

Band	Left helix	Helix$_{3-10}$	β-Sheet	β-Turn	Experimental
A	ν_{as} COO^-	ν_{as} COO^-	ν_{as} COO^-		ν_{as} COO^-
	Amide I			Amide I	
B	Amide I	Amide I	Amide I	ν_{as} COO^-	Amide I
C	ν C (H_2)—C (Imi)	ν C (H_2)—C (Imi)	ν C (H_2)—C (Imi)	ν C (H_2)—C (Imi)	
	Amide II	Amide II	Amide II	Amide II	
		δ_{as} NH_3^+ + ν_s COO^-		δ_{as} NH_3^+ + ν_s COO^-	Amide II
	δ_{as} NH_3^+	δ_{as} NH_3^+	δ_{as} NH_3^+	δ_{as} NH_3^+	δ_{as} NH_3^+
	ν_s COO^-	ν_s COO^-	ν_s COO^-		
				δ_s NH_3^+	
	ν C=N (Imi)	ν C=N(Imi)	ν C=N (Imi)	ν C=N (Imi)	
D	Amide III	Amide III	Amide III	Amide III	
	δ_s CH_2 wagging	δ_s CH_2 wagging	δ_s CH_2 wagging	δ_s CH_2 wagging	Amide III
	δ_s CH_2 (Imi)	ν = C—N (Imi)	ν = C—N (Imi)	δ_s CH_2 (Imi)	Ring vibrations
			ν C—N (Imi)	ν C—N (Imi)	

tive electrostatic interaction between the C terminal of one peptide molecule and the N terminal of another one may induce intermolecular interactions. In fact, the position of band A suggests that the N- and C-terminal groups are close to each other. Second, H-bonding formation between protonated and neutral side chains of different molecules may stabilize the intermolecular β-sheet conformation. At higher pH, the position of the amide I band is slightly shifted toward lower wavenumbers (1665 cm^{-1} at pH 6.0 and 1660 cm^{-1} at pH 8.0), suggesting some distortion of this conformation. The possibility of intermolecular H-bonding between side chains is reduced in going from pH 4.0 to pH 8.0, limiting the stabilization of intermolecular β-structure.

Conclusions

The IR contribution of TFA from unpurified synthetic hexahistidine samples is easily removed by applying a simple subtraction mode based on eliminating the strong absorption bands at 1147 and 1200 cm^{-1}. This correction is performed in two steps. In the first step, the TFA content of the sample is calculated from the absorbance at 1200 cm^{-1}. In the second step, a TFA spectrum at the appropriate concentration is subtracted from the sample spectrum by using a scaling factor to completely remove the strong bands. This correction is performed either in one operation (TFA and buffer contributions are eliminated together) or by subtracting

three times (independent TFA and water removal). Both modes produce a reliable corrected spectrum without either TFA or water contribution. The quality of the experimentally corrected spectrum allows assigning the bands when compared with semiempirical calculated spectra. Although this subtraction strategy was optimized with the histidine peptide, it might be generalized to other unpurified samples.

Acknowledgments

The authors thank CONICET, SeCyT–UNC, and ANPCyT for financial support. L.E.V. thanks CONICET for the fellowship grant. Language assistance by Karina Plasencia is gratefully acknowledged.

References

[1] B. Bacsa, K. Horváti, S. Bõsze, F. Andreae, C.O. Kappe, Solid-phase synthesis of difficult peptide sequences at elevated temperatures: a critical comparison of microwave and conventional heating technologies, J. Org. Chem. 73 (2008) 7532–7542.
[2] N.I. Martin, R.M.J. Liskamp, Preparation of N^G-substituted L-arginine analogues suitable for solid phase peptide synthesis, J. Org. Chem. 73 (2008) 7849–7851.
[3] S.D. Wilking, N. Sewald, Solid phase synthesis of an amphiphilic peptide modified for immobilisation at the C-terminus, J. Biotechnol. 112 (2004) 109–114.
[4] E. Kaiser, J. Rohrer, Determination of residual trifluoroacetate in protein purification buffers and peptide preparations by ion chromatography, J. Chromatogr. A 1039 (2004) 113–117.
[5] V.V. Andrushchenko, H.J. Vogel, E. Prenner, Optimization of the hydrochloric acid concentration used for trifluoroacetate removal from synthetic peptides, J. Pept. Sci. 13 (2007) 37–43.
[6] A. Barth, Infrared spectroscopy of proteins, Biochim. Biophys. Acta Bioenerg. 1767 (2007) 1073–1101.
[7] K.K. Chittur, FTIR/ATR for protein adsorption to biomaterial surfaces, Biomaterials 19 (1998) 357–369.
[8] W.K. Surewicz, H.H. Mantsch, D. Chapman, Determination of protein secondary structure by Fourier transform infrared spectroscopy: a critical assessment, Biochemistry 32 (1993) 389–394.
[9] A. Bertrand, R.M. Brito, A.J. Alix, J.M. Lancelin, R.A. Carvalho, C.F. Geraldes, F. Lakhdar-Ghazal, Conformation study of HA(306–318) antigenic peptide of the haemagglutinin influenza virus protein, Spectrochim. Acta A 65 (2006) 711.
[10] V.V. Andrushchenko, H.J. Vogel, E.J. Prenner, Solvent-dependent structure of two tryptophan-rich antimicrobial peptides and their analogs studied by FTIR and CD spectroscopy, Biochim. Biophys. Acta Biomembr. 1758 (2006) 1596–1608.
[11] S. Mukherjee, P. Chowdhury, F. Gai, Infrared study of the effect of hydration on the amide I band and aggregation properties of helical peptides, J. Phys. Chem. B 111 (2007) 4596–4602.
[12] S.-Y. Lin, T.-F. Hsieh, Y.-S. Wei, PH- and thermal-dependent conformational transition of PGAIPG, a repeated hexapeptide sequence from tropoelastin, Peptides 26 (2005) 543–549.
[13] W.K. Surewicz, H.H. Mantsch, New insight into protein secondary structure from resolution-enhanced infrared spectra, Biochim. Biophys. Acta 952 (1988) 115–130.
[14] E. Goormaghtigh, V. Raussens, J.-M. Ruysschaert, Attenuated total reflection infrared spectroscopy of proteins and lipids in biological membranes, Biochim. Biophys. Acta 1422 (1999) 105–185.
[15] S. Noinville, F. Bruston, C. El Amri, D. Baron, P. Nicolas, Conformation, orientation, and adsorption kinetics of dermaseptin B2 onto synthetic supports at aqueous/solid interface, Biophys. J. 85 (2003) 1196–1206.
[16] K. Sackett, Y. Shai, The HIV fusion peptide adopts intermolecular parallel β-sheet structure in membranes when stabilized by the adjacent N-terminal heptad repeat: a ^{13}C FTIR study, J. Mol. Biol. 350 (2005) 790–805.
[17] M.J. Frisch, G.W. Trucks, H.B. Schlegel, G.E. Scuseria, M.A. Robb, J.R. Cheeseman, J.A. Montgomery, T. Vreven, K.N. Kudin, et al., Gaussian03, Revision B.02, Gaussian, Pittsburgh, PA, 2003.
[18] J.G. Mesu, T. Visser, F. Soulimani, B.M. Weckhuysen, Infrared and Raman spectroscopic study of pH-induced structural changes of L-histidine in aqueous environment, Vibr. Spectrosc. 39 (2005) 114–125.
[19] H. Susi, D.M. Byler, Resolution-enhanced Fourier transform infrared spectroscopy of enzymes, Methods Enzymol. 130 (1986) 290–311.
[20] S. Krimm, J. Bandekar, Vibrational spectroscopy and conformation of peptides, polypeptides, and proteins, Adv. Protein Chem. 38 (1986) 181–364.
[21] M. Wolpert, P. Hellwig, Infrared spectra and molar absorption coefficients of the 20 alpha amino acids in aqueous solutions in the spectral range from 1800 to 500 cm^{-1}, Spectrochim. Acta A 64 (2006) (1800) 987–1001.
[22] A.D. Roddick-Lanzilotta, A.J. McQuillan, An in situ infrared spectroscopic study of glutamic acid and of aspartic acid adsorbed on TiO_2: implications for the biocompatibility of titanium, J. Colloid Interface Sci. 227 (2000) 48–54.
[23] W.C. Wimley, K. Hristova, A.S. Ladokhin, L. Silvestro, P.H. Axelsen, S.H. White, Folding of β-sheet membrane proteins: a hydrophobic hexapeptide model, J. Mol. Biol. 277 (1998) 1091–1110.
[24] A.D. Roddick-Lanzilotta, A.J. McQuillan, An in situ infrared spectroscopic investigation of lysine peptide and polylysine adsorption to TiO_2 from aqueous solutions, J. Colloid Interface Sci. 217 (1999) 194–202.
[25] S. Cai, B.R. Singh, Identification of β-turn and random coil amide III infrared bands for secondary structure estimation of proteins, Biophys. Chem. 80 (1999) 7–20.
[26] M. van de Weert, P.I. Haris, W.E. Hennink, D.J.A. Crommelin, Fourier transform infrared spectrometric analysis of protein conformation: effect of sampling method and stress factors, Anal. Biochem. 297 (2001) 160–169.
[27] L.E. Valenti, C.P. De Pauli, C.E. Giacomelli, The binding of Ni(II) ions to hexahistidine as a model system of the interaction between nickel and His-tagged proteins, J. Inorg. Biochem. 100 (2006) 192–200.